

Do Intermolecular Interactions Control Crystallization Abilities of Glass-Forming Liquids?

K. Kaminski, K. Adrjanowicz,* Z. Wojnarowska, M. Dulski, R. Wrzalik, and M. Paluch

Institute of Physics, Silesian University, ul. Uniwersytecka 4, 40-007 Katowice, Poland

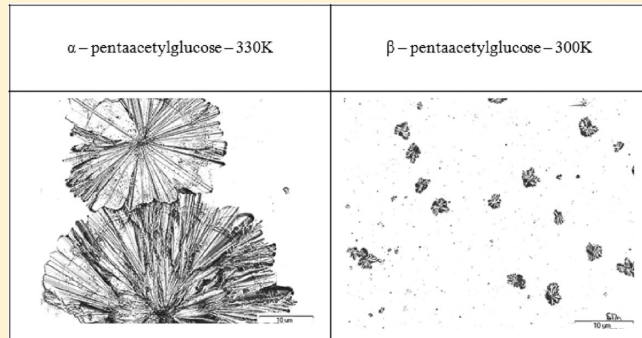
E. Kaminska

Department of Pharmacognosy and Phytochemistry, Medical University of Silesia, ul. Jagiellonska 4, 40-007 Sosnowiec, Poland

A. Kasprzycka

Silesian University of Technology, Department of Chemistry, Division of Organic, Chemistry, Biochemistry and Biotechnology, ul. Krzywoustego 4, 44-100 Gliwice, Poland

ABSTRACT: Broadband dielectric spectroscopy was used to investigate molecular dynamics of three very similar systems: D-glucose, α -pentaacetylglucose, and β -pentaacetylglucose in a wide range of temperatures. We found out that two latter systems (differing only in location of the acetyl group attached to the first carbon in the sugar ring) reveal completely opposite tendencies to crystallization. Therefore, the aim of this Article was to investigate in detail molecular dynamics of both pentaacetylglucoses to assess what are the underlying of different crystallization abilities of so closely related carbohydrates. To analyze the kinetics of crystallization, we used Avrami and Avramov approaches. Interestingly, we found out that both α -and β -pentaacetylglucose exhibit completely different crystallization mechanisms. In the first case, the value of Avrami exponent was estimated to be $n = 2$, whereas for the second carbohydrate this exponent was equaled to $n = 5.5$. Additionally, we have carried out isothermal time-dependent dielectric measurements on D-glucose to demonstrate that this saccharide is more stable than its acetyl derivatives. Results presented in this Article indicate that besides molecular mobility, the character of the intermolecular interactions might also be another important factor governing crystallization process. Surprisingly, this issue is not often addressed during studies on crystallization abilities of different glass-formers. Finally, additional optical measurements were carried out to get more detailed information about nucleation density, activation barrier for a crystal growth, and morphology of crystallization structures.



INTRODUCTION

During cooling of liquid below its melting temperature, there are two different scenarios possible. In the first one, supercooled liquid crystallizes, whereas in the second one, it reaches a glassy state. Therefore, a tremendous number of studies have been carried out to understand why some liquids exhibit greater glass-formation abilities, whereas the others cannot be very easily supercooled below the glass-transition temperature. A few years ago, it was commonly believed that the ability of glass-formers to crystallize is mainly due to competition between the rate of supercooling and crystal growth.^{1,2} One of the consequences of this paradigm was a common persuasion that all liquids can be vitrified if only sufficiently fast cooling rate is applied.

From the classical point of view, crystallization rate can be written as follows^{3,4}

$$G(T) = f(T)/D(T) \quad (1)$$

where $D(T)$ represents temperature dependences of molecular diffusion and $f(T)$ is nucleation free energy term. The latter quantity can be evaluated from

$$\Delta F = \frac{16\pi\gamma^3}{3\delta\mu^2} \quad (2)$$

where γ is interfacial tension between supercooled liquid and crystal and $\delta\mu$ is the difference in free energy per unit volume between them. Because

$$\delta\mu \approx \Delta H_f(1 - T/T_m) \quad (3)$$

Received: March 13, 2011

Revised: August 30, 2011

Published: August 30, 2011

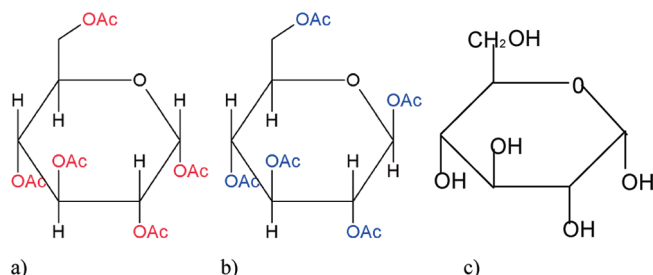
where ΔH_f is enthalpy of fusion and T_m is melting temperature, one can obtain that thermodynamic driving force increases with a degree of supercooling and strongly depends on to the enthalpy of fusion.

Crystallization rate is also dependent on $D(T)$, which can be related to τ_v defining characteristic time of material transport. It is believed that τ_t is equal to the structural relaxation time τ_α . One can also add that τ_α is connected to the viscosity via Maxwell model

$$\tau_\alpha = C\eta/G \quad (4)$$

where η is viscosity and G is the high-frequency shear modulus. It is usually equal to 2 GPa for organic liquids and $C = 1$.¹³ However, recent findings have indicated that material

Scheme 1. Chemical Structures of α -Pentaacetylglucose (a), β -Pentaacetylglucose (b), and Non-Modified D-Glucose (c)



transport decouples from the viscosity or structural relaxation at certain temperature T_B , which is usually equal to $1.2T_g$.^{5–9} It is worth noting that Swallen et al. showed that enhancement of the translational diffusion can be even greater by a factor of 400 than viscosity at the glass-transition temperature.¹⁰ Consequently, the crystal growth rate is faster than that predicted from the viscosity data. Hence, it was concluded that

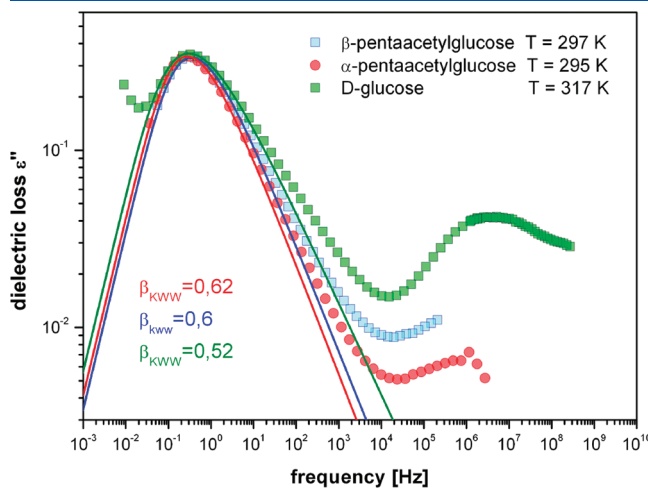


Figure 2. Superimposed α -loss peaks measured of D-glucose (green filled squares), α -pentaacetyl glucose (filled red circles), and β -pentaacetylglucose (cyan filled squares) at indicated temperatures. Solid lines represent the best β_{KWW} fits to the data.

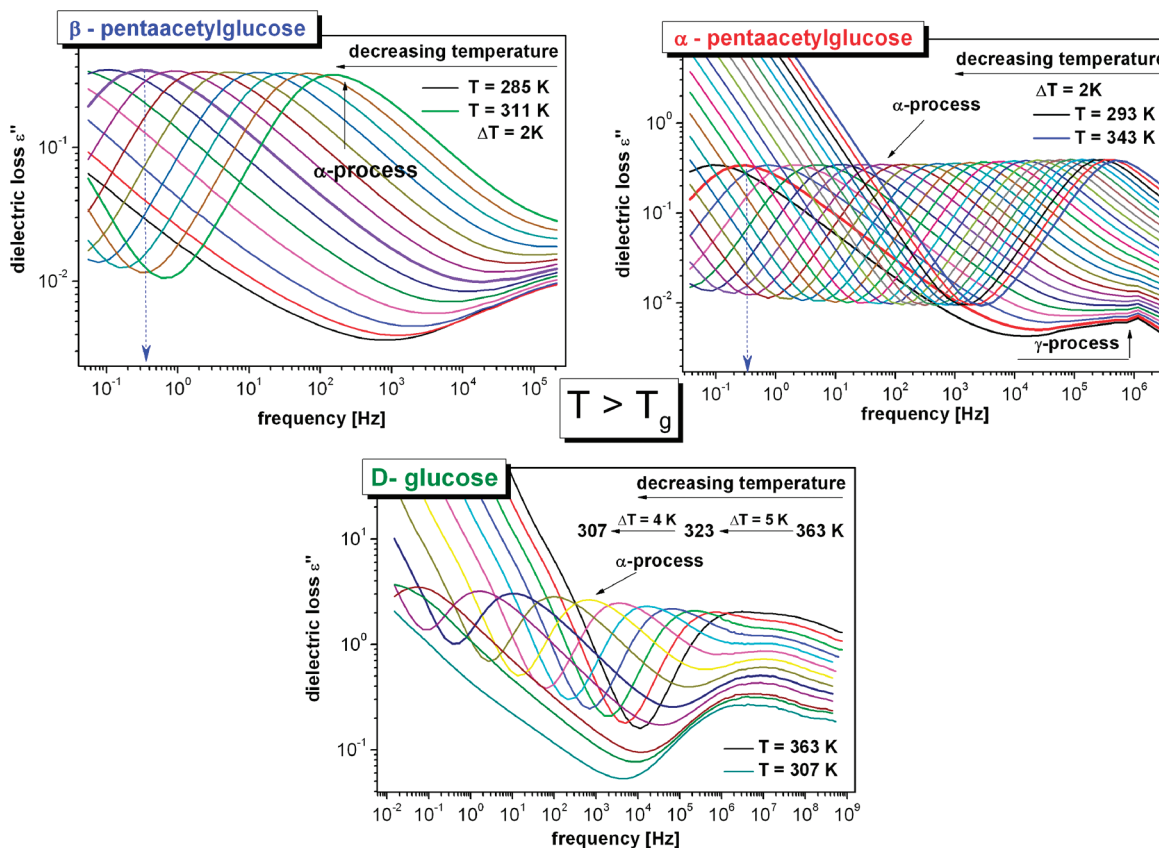


Figure 1. Dielectric loss spectra measured above the glass-transition temperature for α - and β -pentaacetylglucoses and D-glucose.

crystallization kinetics below T_B is controlled mainly by translational diffusion, whereas above T_B reorientational diffusion (viscosity or structural relaxation process) governs crystallization kinetics.^{5,10,11} In this context, it should be mentioned that decoupling between η and D_T usually correlates with the fragility^{8,9,12} being a measure of deviation of the temperature dependence of the structural relaxation times from the Arrhenius behavior of the glass-forming liquid. It was observed that the more fragile the liquid, the greater the decoupling between D_T and viscosity. In a recent paper by Ediger et al.,¹³ dependence of the crystallization kinetics (μ_c)

versus viscosity has been studied. They found the following phenomenological relation

$$\mu_c = \eta^{-\xi} \quad (5)$$

where ξ is an exponent lying in the range $(0 \leq \xi \leq 1)$. Therein, it was shown that the lower value of exponent, the greater decoupling between viscosity and translational diffusion occurs. As a consequence, crystallization process was much faster.

The other theoretical approach emphasizing the role of fragility in crystallization abilities of glass-forming liquids is two-order parameter (TOP) model proposed by H. Tanaka.^{14–16} He claimed that liquid–glass transition is an effect of the competition between long-range density ordering leading to the formation of the crystals and short-range bond ordering favoring the formation of the locally preferred structures not consistent with the geometry of crystals. When the latter effect dominates, the system becomes frustrated, and inhibition of the crystallization rate is expected. It was also assumed that the measure of degree of frustration is fragility, that is, greater fragility (the lower frustration), implying greater crystallization ability of glass formers. Recent high-pressure studies seem to confirm this supposition.^{17,18} It was also demonstrated that for polymers the tendency to crystallization increases with increasing fragility.¹⁹

In this Article, we present dielectric studies on crystallization kinetics in three carbohydrates nonmodified D-glucose and α - and β -pentaacetylglucoses. We will show that despite the great similarity in chemical structure and molecular dynamics of the two latter systems, they differ completely in crystallization abilities. By comparing molecular dynamics of examined herein carbohydrates, we are able to certify that not only the fragility plays an important role in crystallization tendencies of the samples but

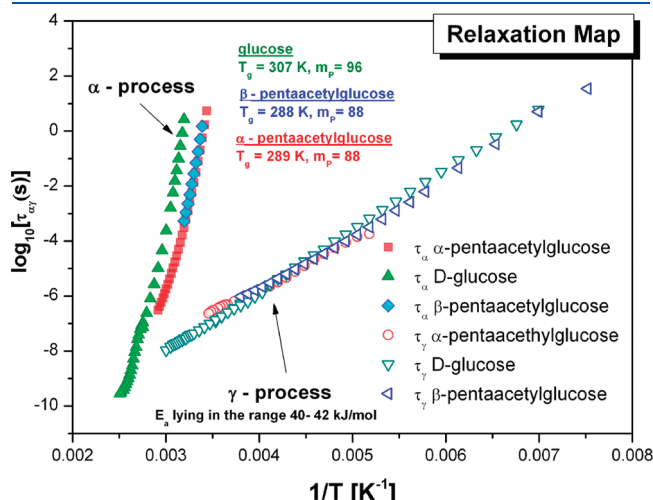


Figure 3. Relaxation map of D-glucose and α - and β -pentaacetylglucoses.

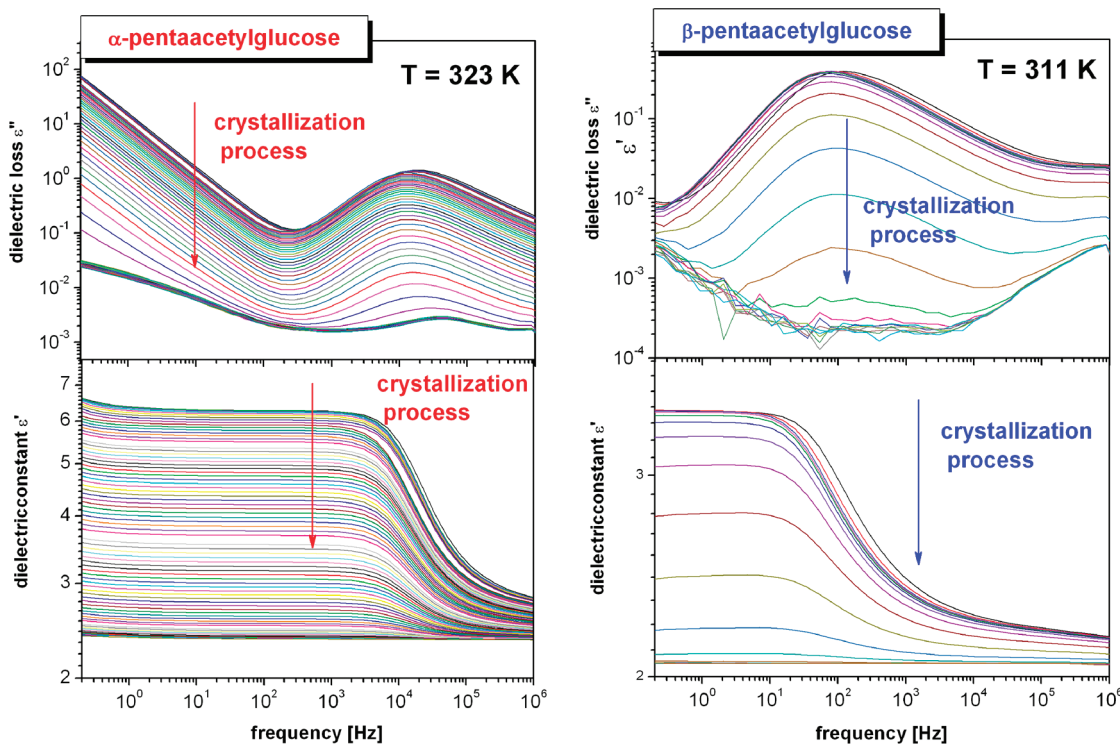


Figure 4. Representative dielectric loss (upper panels) as well as dispersion spectra (lower panels) measured for α - and β -pentaacetylglucoses at the indicated temperatures during crystallization process.

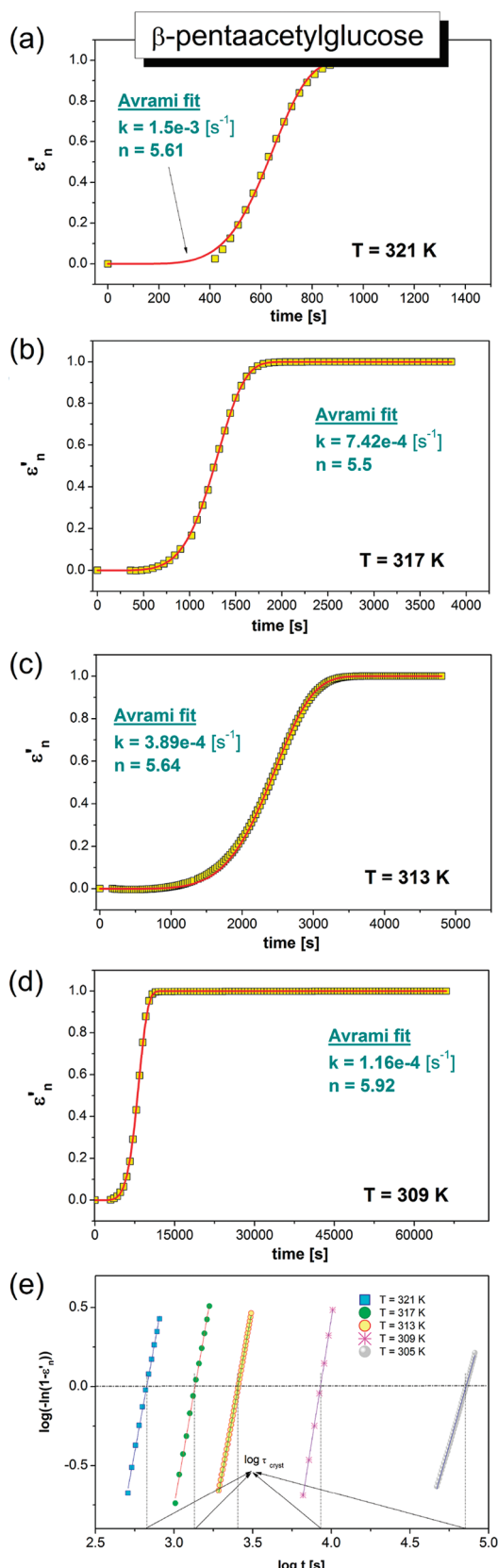


Figure 5. Time evolutions of the normalized constant for the measurements carried out at $T = 321$ (a), 317 (b), 313 (c), and 309 K (d). Solid lines are the best Avrami fits. (e) Avrami plot for β -pentaacetylglucose. In this Figure, only data relative to a normalized dielectric constant varying between 0.2 and 0.9 are shown.

also that the character of intermolecular interactions might be responsible for it as well.

EXPERIMENTAL SECTION

D-Glucose of purity greater than 99% was supplied from Sigma Aldrich, whereas α - and β -pentaacetylglucoses were synthesized for the purpose of this Article. (Chemical structures are shown in Scheme 1.) The purity of the samples was determined to be higher than 99%. One can add that both pentaacetyl derivatives were synthesized in the same environment and with the use of the same procedure. The synthetic procedure is described below. It should also be stressed that each sample was tested by NMR spectroscopy to confirm that purity of the molten and crystalline samples is the same.

Isobaric dielectric measurements at ambient pressure were carried out using a Novo-Control alpha dielectric spectrometer (10^{-2} to 10^7 Hz). The samples were placed between two stainless-steel flat electrodes of the capacitor with gap 0.1 mm. The temperature was controlled by the Novo-Control Quattro system, with use of a nitrogen-gas cryostat. Temperature stability of the samples was better than 0.1 K.

The optical measurements on the crystal growth were carried out using Olympus BX51 polarized microscope, equipped with an Olympus SC30 camera and a halogen source light. It should be mentioned that the procedure of measurements was the same as that in the case of dielectric measurements. Optical figures were collected using Olympus Soft Imaging Solutions GmbH 5.1 (analysis getIT software) at UMPlanFI $10\times$ objective and at 0.30 aperture. Additionally, all stored Figures were corrected using Adobe Photoshop 12 software.

Synthesis Procedure. 1,2,3,4,6-Penta-O-acetyl- β -D-glucose and 1,2,3,4,6-penta-O-acetyl- α -D-glucose were obtained by the same procedure described in ref 36. Structures of both anomers and their purity (α 99%, β 99%) were confirmed by nuclear magnetic resonance spectra.

RESULTS

Isobaric Dielectric Measurements. In Figure 1, dielectric loss spectra of α - and β -pentaacetylglucoses and nonmodified glucose are presented. In each case, structural relaxation process can be observed above the glass-transition temperature. This process shifts toward lower frequencies with decreasing temperature. However, it can be seen that in the case of α - and β -pentaacetylglucose we were able to follow the structural relaxation process in a wide range of temperatures, while in non-modified D-glucose this mode was observed only at temperatures at which its f_{\max} was below 200 Hz. It can be also seen that β anomer starts to crystallize very quickly above $T = 313$ K. Hence, at the first sight it is obvious that α - and β -pentaacetylglucoses reveal completely different glass-formation abilities. The other very interesting observation is that the contribution of dc conductivity to the loss spectra of pentaacetyl derivatives is considerably smaller with respect to D-glucose. It is related to the fact that D-glucose forms networks connected via the hydrogen bonds. Therefore, there are many channels for proton migration in this compound. In modified saccharides, proton hopping has been inhibited because all hydrogen bonds were destroyed. Hence, the proton hopping is the most probable explanation for a difference in dc conductivity between investigated herein samples.

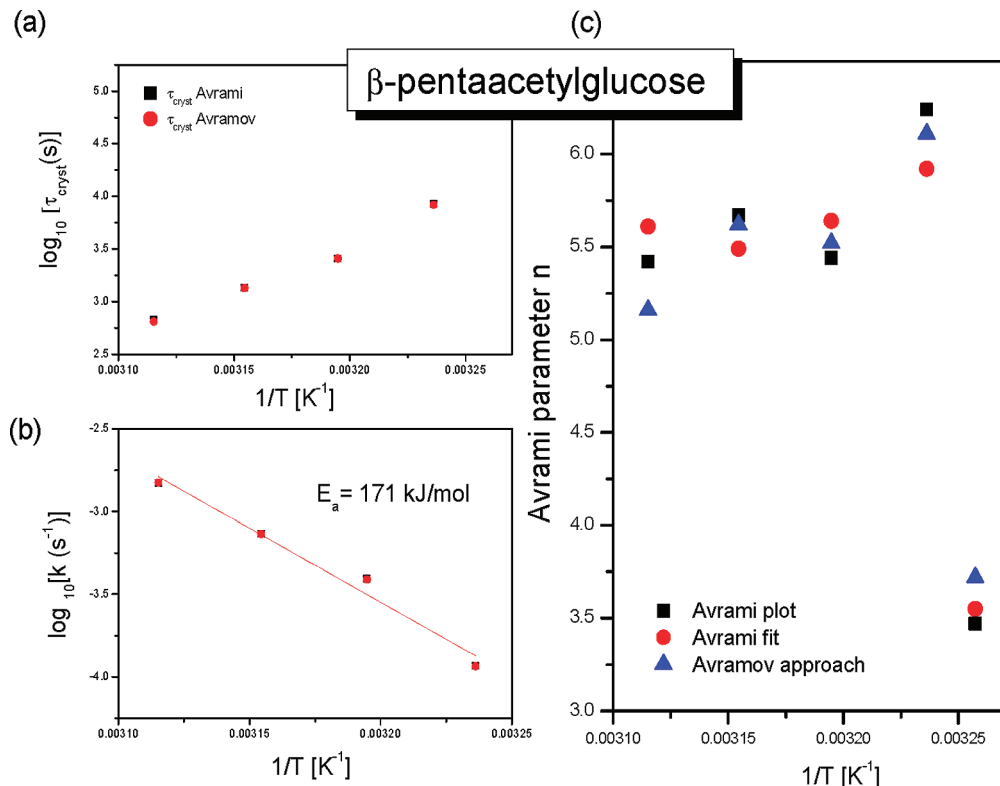


Figure 6. (a) Temperature dependence of crystallization time (τ_{cryst}) estimated via Avrami (filled black squares) and Avramov (filled red circles) approaches. (b) Temperature dependence of constant rate k . Solid line represents Arrhenius fit. (c) Temperature dependence of the Avrami exponent estimated from Avrami fit (red filled circle), Avrami plot (black filled squares), and Avramov approach (blue filled triangles).

In Figure 2, superimposed dielectric loss spectra of all investigated herein carbohydrates are presented. It should be noted that structural dispersion peaks of D-glucose and α -pentaacetylglucose were slightly shifted vertically and horizontally to have the same τ_α as β -pentaacetylglucose. Next, α -relaxation peaks were fitted to the one-sided Fourier transform KWW function²⁰

$$\phi(t) = \exp[-(t/\tau_\alpha)^\beta] \quad (6)$$

with stretching exponent equal to $\beta_{\text{KWW}} = 0.52$ (D-glucose), $\beta_{\text{KWW}} = 0.6$ (β -pentaacetylglucose), and $\beta_{\text{KWW}} = 0.62$ (α -pentaacetylglucose). The broadest dispersion of the structural relaxation process is found for D-glucose. Therefore, one can state that the most heterogeneous sample of all studied by us is D-glucose. This result can be explained in view of the formation of different networks by this carbohydrate. The other very interesting observation is that both modified carbohydrates have only slightly different values of stretching exponent. One can remember that in the case of D- and L- arabinoses (they have almost the same chemical structure) we observed a very similar scenario.²¹

To determine parameters characterizing molecular dynamics of the supercooled and glassy states of all samples investigated herein, we analyzed their structural and secondary relaxation processes with the use of the Havriliak–Negami function.²² Temperature dependences of α -relaxation times were fitted to the commonly used Vogel–Fulcher–Tammann–Hesse (VFTH) equation (Figure 3)²³

$$\tau_\alpha = \tau_0 \exp\left(\frac{D_T T_0}{T - T_0}\right) \quad (7)$$

whereas secondary relaxation processes were described by the Arrhenius power law

$$\tau_\gamma = \tau_0 \exp(E_a/k_B T) \quad (8)$$

From the extrapolation of VFTH fits, one can estimate glass-transition temperature of D-glucose ($T_g = 307$ K) and α - and β -pentaacetylglucose ($T_g = 289$ and 288 K, respectively). The glass-transition temperature T_g was defined as the temperature at which structural relaxation times is equal to 100 s. It is clearly visible that both latter carbohydrates have almost the same glass-transition temperatures, being almost 20 K lower than that estimated for D-glucose. One can add that this result is consistent with the general rule that hydrogen bonding systems have higher melting, boiling, as well as glass-transition temperatures.

Because recent papers indicate that fragility is an important parameter controlling the crystallization ability of the given glass former, we have calculated the steepness index using the definition

$$m = d \log_{10} \tau_\alpha / d(T_g/T)|_{(T_g/T)=1} \quad (9)$$

As a result, we obtained $m = 96$ (D-glucose) and 88 for both modified glucoses. Hence, it is evident that elimination of the hydrogen bonds makes the given system less fragile. An interesting fact is that both pentaacetylglucoses are characterized by the same fragility. As it can also be seen from the relaxation map (Figure 3), secondary relaxation processes in

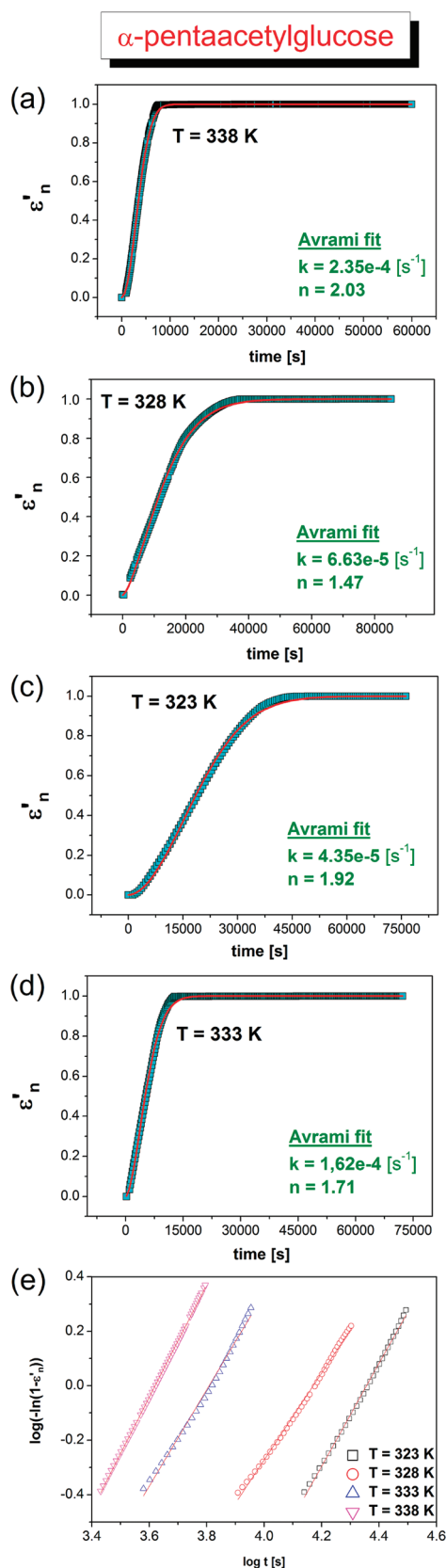


Figure 7. Time evolutions of the normalized constant for the measurements carried out at the indicated temperatures. Solid lines are the best Avrami fits. (e) Avrami plot of the data obtained for α -pentaacetylglucose. It should be noted that only data relative to a normalized dielectric constant varying between 0.2 and 0.9 are shown.

each carbohydrate have almost the same relaxation time at given temperature. Moreover, activation energies determined from the Arrhenius equation are almost the same as those for the observed secondary modes. However, this issue was addressed elsewhere.²⁴

Summarizing this part, we can certify that both pentaacetylglucoses are characterized by almost the same molecular dynamics. It is well seen that hydrogen bonds influence dynamics of the supercooled phase in D-glucose.

Analysis of Crystallization Process. In Figure 4, time-dependent dielectric loss and dispersion spectra measured for α - and β -pentaacetylglucoses at $T = 323$ and 311 K, respectively, are presented. We can observe that in both cases dielectric strength as well as static epsilon decrease with time. Such pattern of behavior is characteristic for the crystallization process. To describe crystallization kinetics in both pentaacetylglucoses, we analyzed static epsilon. One can add that accordingly to the Onsager relation^{25,26} ϵ_0 is proportionally related to the number of relaxing dipoles and square of dipole moment

$$\epsilon_0 \approx N\mu^2 \quad (10)$$

Therefore, as the crystallization process proceeds, the number of relaxing molecules decreases. This in turn provides direct information about an extent of crystallization process.

Isothermal crystallization of α - and β -Pentaacetylglucose. First, in each case, we chose static epsilon measured at a frequency that was not being affected by the contribution from the polarization of the plates. Then, our data were normalized using following formula

$$\epsilon'_n' = \frac{\epsilon'(0) - \epsilon'(t)}{\epsilon'(0) - \epsilon'(\infty)} \quad (11)$$

In Figure 5a–d, variation of ϵ'_n' versus time at indicated temperatures is presented. It can be seen that as the temperature decreases, the crystallization process becomes slower. However, we also noted that there is an enormous difference in the speed of crystallization between measurements carried out at $T = 307$ and 309 K, probably indicating a change in the mechanism of crystallization.

To analyze isothermal crystallization kinetics, we used standard Avrami approach^{27,28}

$$1 - \varphi_c = \exp(-kt^n) \quad (12)$$

where φ_c is the crystalline volume fraction, k is a constant given by the temperature and the geometry of the sample, and n is the Avrami exponent. The value of the last parameter is very often correlated to the dimensionality of the process. Because φ_c can be identified to dielectric ϵ'_n , one can use this equation directly to fit the data presented in Figure 5a–d. The solid lines are the best Avrami fits. It is visible that the accuracy of the Avrami fit to the experimental data is very good in each case. Surprisingly, we have found that parameter n , which gives us information about dimensionality or mechanism of crystallization process, is greater than 5. It is quite surprising because many experimental studies have shown that this parameter lies within the range of $n = 2$ to 3 .²⁹ Of course in the literature one can find systems for which n parameter was greater than 3, but it is not so common.³⁰ Unfortunately, we cannot explain why Avrami exponent is so high in that case.

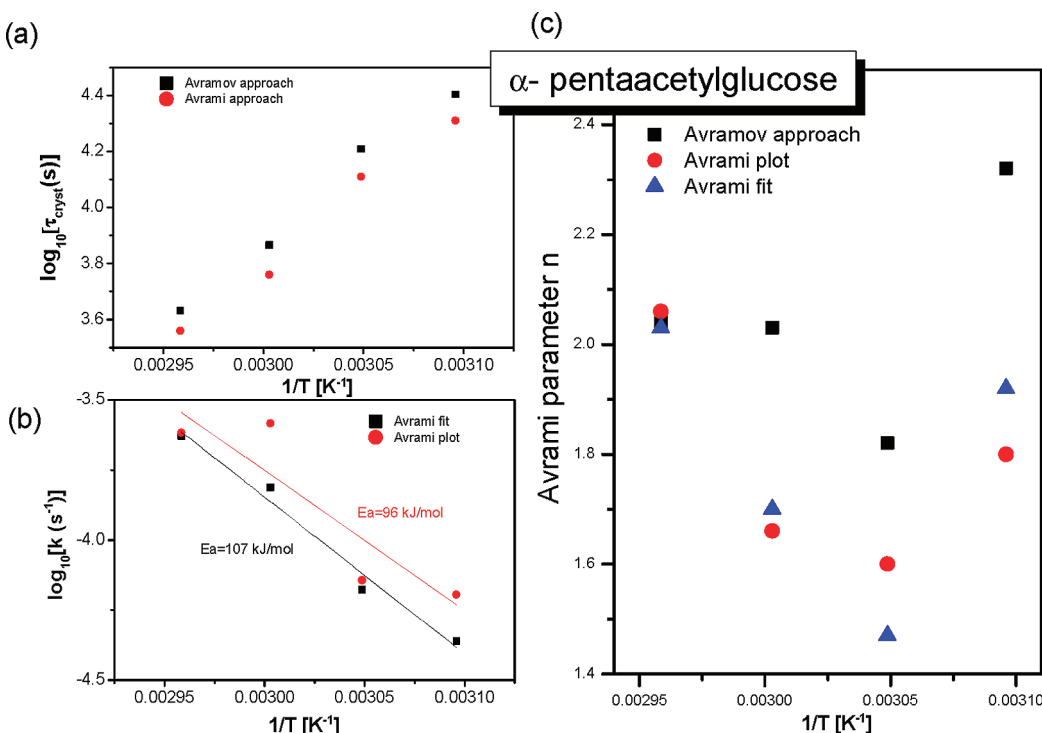


Figure 8. (a) Temperature dependence of crystallization time (τ_{cryst}) estimated via Avrami (filled red circles) and Avramov (filled black squares) approaches. (b) Temperature dependence of constant rate k estimated from Avrami fit and plot. Solid lines represent Arrhenius fits. (c) Temperature dependence of the Avrami exponent (n) estimated from Avrami fit (blue filled triangles), Avrami plot (red filled circle), and Avramov (black filled squares) approaches.

To be sure of the correct estimation of n and constant rate k , we have applied another approach.^{27,28} To do that we need to reproduce data in double logarithmic representation first, $\log(-\ln(1 - \varepsilon_n'))$ versus $\log t$ (Figure 5e). Then, by fitting this dependence to the linear function, we obtain n as a slope and $\log k$ as an intercept with the y axis. Moreover, from this plot one can also obtain τ_{cryst} , which can be attributed to the projection on the x axis of the straight line for which $y(\varepsilon_n) = 0$ (Figure 5e). To verify correctness of the estimation of n and k , we also applied a method proposed by Avramov (data not shown).³¹ Interestingly we found out that values of both parameters are in quite good agreement with those previously obtained. In Figure 6, we have presented all important results derived from the analysis of isothermal crystallization data with the use of Avrami and Avramov approaches. It can be seen that irrespective of the method of analysis, the values of n , k , or τ_{cryst} are comparable. One can add that similar conclusions were also derived by other researchers.^{32,33}

To estimate the activation energy for crystallization in β -pentaacetylglucose, we have plotted the constant rates k obtained from the Avrami fits versus reciprocal temperature. As a result, we obtained $E_a = 171 \text{ kJ/mol}$. In Figure 7, the analysis of crystallization data obtained for the second modified carbohydrate, α -pentaacetylglucose, is shown. It should be noted that to estimate the constant rate, Avrami exponent n , and τ_{cryst} the same procedures as those in the case of β -pentaacetylglucose were applied. However, one can add that in α -pentaacetylglucose measurements were carried out at higher temperatures $T = 323\text{--}338 \text{ K}$. It was related to the experimental finding that between $T = 309$ and 321 K crystallization time was much longer than that estimated for β anomer. In Figure 8, all results derived from the analysis of the isothermal crystallization data are pre-

sented. As it can be seen, there are differences among values of n , k , and τ_{cryst} estimated via different methods. However, these discrepancies are not so large to be considered. It is worth noting, that Avrami exponent $n \approx 2$ is much smaller than that estimated for β isomer. Therefore, it is clear evidence that the mechanism of isothermal crystallization in both compounds investigated herein is completely different. Moreover, crystallization times $\tau_{\text{cryst}} = 676$ and $20\,417 \text{ s}$ estimated for measurements carried out at $T = 321$ and 323 K for β - and α -pentaacetylglucoses, respectively, differ significantly. This is the next experimental proof that α -pentaacetylglucose is more stable against crystallization than β anomer.

In addition, just as in the case of β -pentaacetylglucose, the activation energy for the crystallization process of α -isomer was determined. (See Figure 8b.) We obtained $E_a = 107$ or 96 kJ/mol depending on the method of determination of constant rate $k [\text{s}^{-1}]$. It should be stressed that the former and latter values of E_a were obtained when we use k determined from the Avrami plots and fits, respectively. One should remember that for less thermally stable β isomer, $E_a = 171 \text{ kJ/mol}$ was obtained. Therefore, it is well-demonstrated that activation barrier for the less stable system is almost two times greater than that evaluated for α anomer. At the first sight, this result seems to be quite surprising. However, one needs to bear in mind that the crystallization process is generally governed by nucleation and crystal growth barrier, which are likely to have different activation energies.³⁴ At this place, one needs to state that from the dielectric measurements one evaluates the activation energy of crystallization being a sum of nucleation and crystal growth barrier. Because β isomer is less stable than the α anomer, one could expect that the nucleation barrier should be much

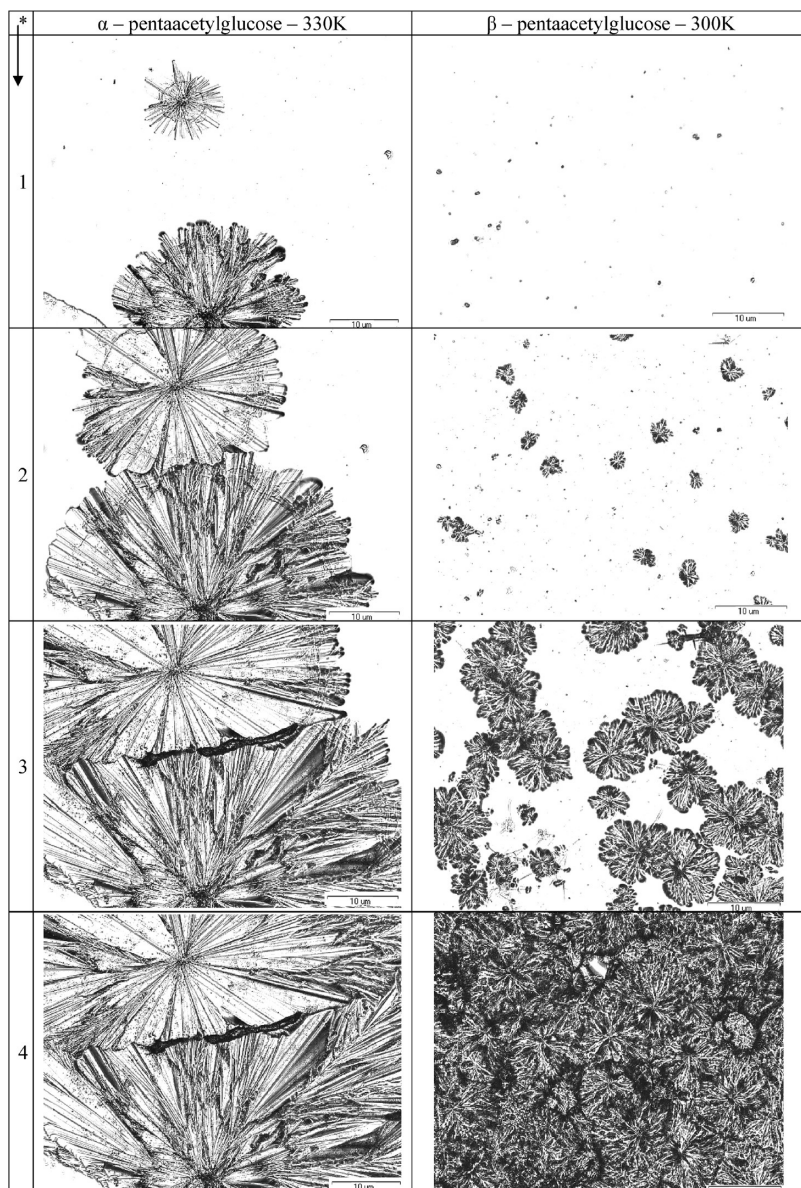


Figure 9. Crystallization snapshots monitored under microscope.

lower in the case of the former carbohydrate. Therefore, the energy of nucleation must determine greater stability of the α anomer.

Crystallization Kinetics under Microscope. To get more detailed information about crystallization mechanism, nucleation density, or activation barrier for the crystal growth in both modified saccharides, additional measurements with the use of the optical microscope have been carried out. First, we have performed time-dependent isothermal experiments at different temperatures. As can be seen in Figure 9, α - and β -pentaacetyl glucoses differ significantly in the density nucleation. We obtained that there are around 1 to 2 and 30 centers of nucleation per $4900 \mu\text{m}^2$, respectively, in the former and the latter saccharides. It is worth pointing out that the number of nuclei did not change with temperature. Additionally, we also found out that both modified compounds form completely different crystallization structures. One can add that crystals of β pentaacetyl

glucose radiate symmetrically outward from a central point in small divergent blended crystals ($\sim 20 \mu\text{m}$ diameter) without producing stellar forms in the crystallization process. Crystals of α -anomer radiate stellate (star-like) in the form of relatively big (about some mm diameter) tabular or blended crystals in the first stage of the crystallization process and the fibrous forms in the second stage. Hence, this finding can explain the difference in Avrami exponent estimated from dielectric measurements carried out for α - ($n = 2$) and β - ($n = 5$) pentaacetylglucoses. It should be also mentioned that the morphology of crystal did not change with temperature.

Because isothermal crystallization curves have been measured at different temperatures for both investigated saccharides, the induction times of crystallization as well as apparent activation barriers for the crystals growth E_{cg} can be estimated. In Figure 10a,b, the length of the crystals is plotted as a function of time for both anomers. Now, in contrast with the dielectric measurements,

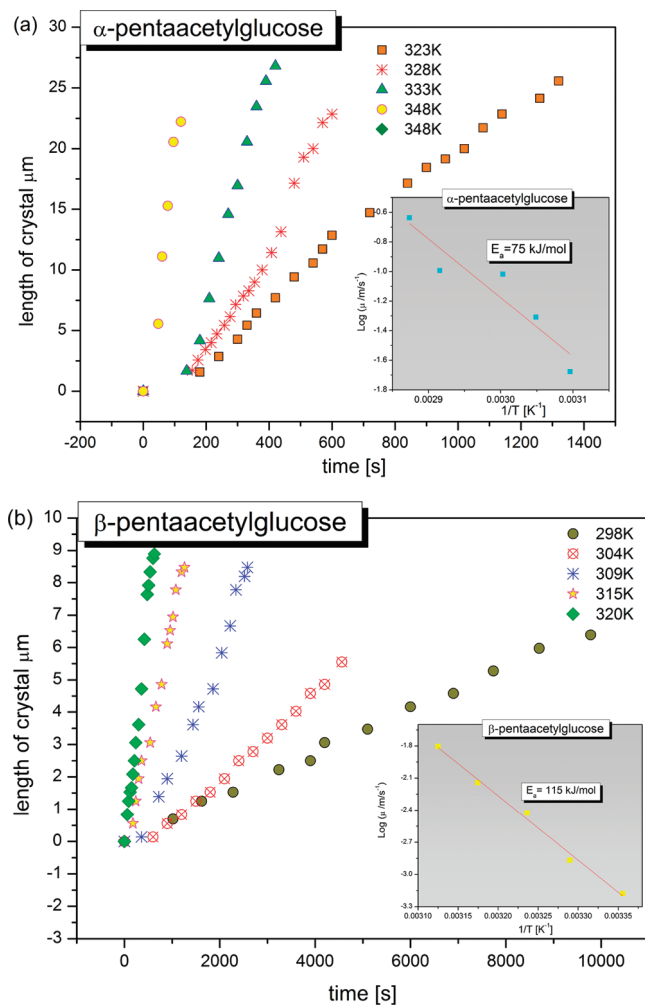


Figure 10. Dependence of length of crystal versus time measured for α (panel a) and β anomer (panel b). In the insets, crystal growth rates are plotted as a function of reciprocal temperature. The solid lines are the best Arrhenius fits.

crystallization curves are linear. One can add that this type of behavior is typical for the crystal growth controlled by interface kinetics. To calculate E_{cg} , one needs to estimate crystal growth rates (μ_r) that can be evaluated from the slope of dependences presented in Figure 10. Next, $\log \mu_r$ was plotted as a function of reciprocal temperature; see Figure 10 insets. Having dependences $\log \mu_r$ versus $1/T$, the apparent activation barriers for the crystal growth were estimated. From the fitting we obtained, $E_{cg} = 75$ and 116 kJ/mol for α and β isomer, respectively. It can be seen that these activation barriers are much smaller than those estimated from dielectric measurements. However, it should be mentioned that E_a calculated from dielectric measurements is rather a sum of the activation energy for the nucleation and the crystal growth. Therefore, it is natural to expect that the activation barrier for the crystallization, accounting for only the latter contribution, determined from the optical studies is much smaller.

In the previous part of this Article, it was claimed that both pentaacetylglucoses must differ in the activation barrier for the nucleation. However, it is very difficult to estimate this quantity. Therefore, because of that reason we have chosen another way to

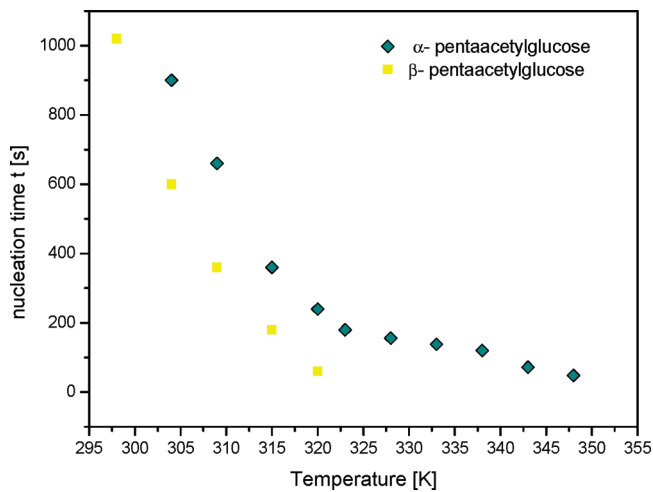


Figure 11. Temperature dependence of the induction time (time of appearance of the nuclei).

visualize difference in nucleation between both investigated isomers. In Figure 11, dependence of the induction time (appearance of the nuclei) for the crystallization is presented as a function of temperature. This simple graph is the best illustration that activation barrier for the nucleation is surely greater in the case of α -pentaacetyl glucose. Moreover, taking into account results presented in Figure 11, one can state that the formation of the nuclei is much faster in the case of β isomer at a given temperature.

DISCUSSION

In Figure 12, time-dependent isothermal loss spectra of nonmodified D-glucose measured at $T = 343$ and 363 K were presented. As can be seen, dielectric strength of structural relaxation process does not change with time. This is a clear indication that this carbohydrate does not crystallize and is the most stable of all investigated herein carbohydrates. Moreover, measurements with the use of the microscope confirmed that D-glucose is very stable in the supercooled liquid state. Hence, one can ask, "What is the origin of greater stability of D-glucose in comparison to its pentaacetyl derivatives?". On the basis of the dynamical parameters determined from dielectric measurements for all three systems, one can suppose that neither fragility nor cooperativity, reflected in stretching exponent, govern crystallization kinetics. It should be mentioned that D-glucose is a highly associating liquid. One can devote readers to the paper by Sidebottom, who showed that glucose forms clusters.³⁵ Therefore, one can postulate that intermolecular interactions might play very important role in stabilization of the supercooled D-glucose. Furthermore, we suppose that in fact hydrogen bonds are responsible for the greater physical stability of nonmodified supercooled saccharides. One can add that it is expected that highly hydrogen bonding systems will exhibit lower tendencies to crystallization irrespective of the fragility or dynamical heterogeneity of the systems. In fact, it is well-documented in the literature that materials that reveal hydrogen-bonding abilities such as saccharides, mono- and polyalcohols, and of polypropylene glycol exhibit low tendency to crystallization and can be classified as rather stable glass-formers.

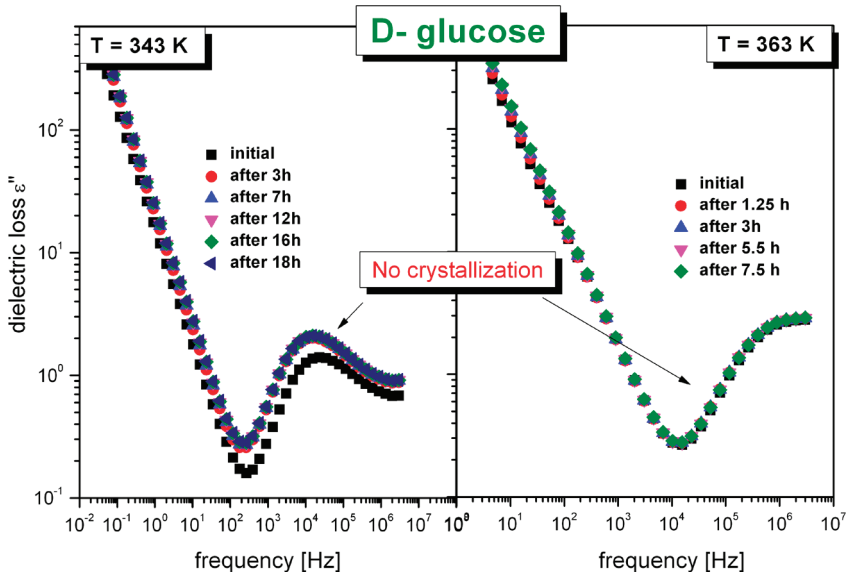


Figure 12. Time-dependent dielectric loss spectra measured for D-glucose at two indicated temperatures.

CONCLUSIONS

In this Article, molecular dynamics of D-glucose and its derivatives, α -pentaacetylglucose and β -pentaacetylglucose, was investigated. As we found out, there are no significant differences in dynamical properties of α -pentaacetylglucose and β -pentaacetylglucose. Both systems have almost the same glass-transition temperatures, fragilities, and stretching exponent. It was demonstrated that D-glucose is more fragile with respect to its modified derivatives. What is more, distribution of relaxation times of the primary relaxation process in D-glucose are greater in comparison with those of the acetyl samples. This implies greater dynamical heterogeneity in the former carbohydrate. We have also found out that D-glucose is the most stable system of all those studied herein. It does not crystallize even at very high temperature and annealed for more than 20 h. Our findings indicate that besides molecular mobility and thermodynamic driving forces, intermolecular interactions might also control crystallization abilities of different glass-formers. Therefore, we expect that network-forming systems will exhibit greater glass-formation abilities.

In this Article, we have also carefully investigated crystallization kinetics in supercooled α - and β -pentaacetylglucoses. Surprisingly, the mechanism of crystallization in both systems along with their tendencies to crystallization are completely different. It appears that α anomer is more stable than β anomer. Moreover, measurements with the use of the microscope showed that both isomers differ in morphology of crystals, activation barrier for the crystal growth, and nucleation density. We also found that E_a for the crystallization determined from the dielectric measurements is much greater than that estimated from the optical studies. Finally, it was also shown that E_a of crystallization obtained for less-stable β isomer is much greater than that calculated for α anomer from dielectric measurements. We conjecture that the activation energy for the nucleation must be much greater in α -pentaacetylglucose than in β -pentaacetylglucose. Data taken under the microscope seem to confirm this supposition.

AUTHOR INFORMATION

Corresponding Author

*E-mail: Kadrjano@us.edu.pl.

ACKNOWLEDGMENT

We are thankful for the financial support of their research within the framework of the project entitled "From Study of Molecular Dynamics in Amorphous Medicines at Ambient and Elevated Pressure to Novel Applications in Pharmacy (contract no. TEAM/2008-1/6)" which operates within the Foundation for Polish Science Team Programme and is cofinanced by the EU European Regional Development Fund.

REFERENCES

- (1) Turnbull, D.; Cohen, M. H. *J. Chem. Phys.* **1958**, *29*, 1049–1054.
- (2) (a) Angell, C. A. *J. Phys. Chem. Solids* **1988**, *49*, 863–871. (b) Angell, C. A. *J. Non-Cryst. Solids* **1991**, *13*, 131–133.
- (3) Magill, J. H.; Li, H. M. *J. Cryst. Growth* **1973**, *20*, 135–144.
- (4) Debenedetti, P. G. *Metastable Liquids*; Princeton University Press: Princeton, NJ, 1997.
- (5) Ngai, K. L.; Magill, J. H.; Plazek, D. J. *J. Chem. Phys.* **2000**, *112*, 1887–1892.
- (6) Donth, E. *The Glass-Transition*; Springer-Verlag: Berlin, 2001.
- (7) Angell, C. A.; Ngai, K. L.; McKenna, G. B.; McMillan, P. F.; Martin, S. W. *J. Appl. Phys.* **2000**, *88*, 3113–3157.
- (8) Sillescu, H. *J. Non-Cryst. Solids* **1999**, *243*, 81–108.
- (9) Ediger, M. D. *Annu. Rev. Phys. Chem.* **2000**, *51*, 99–128.
- (10) Swallen, S. F.; Bonvallet, P. A.; McMahon, R. J.; Ediger, M. D. *Phys. Rev. Lett.* **2003**, *90*, 015901.
- (11) Masuh, A.; Waniuk, T. A.; Busch, R.; Johnson, W. L. *Phys. Rev. Lett.* **1999**, *82*, 2290.
- (12) Tanaka, H. *Phys. Rev. E* **2003**, *68*, 011505.
- (13) Ediger, M. D.; Harowell, P.; Yu, L. *J. Chem. Phys.* **2008**, *128*, 034709–034714.
- (14) Tanaka, H. *J. Chem. Phys.* **1999**, *111*, 3163–3175.
- (15) Tanaka, H. *J. Non-Cryst. Solids* **2005**, *351*, 678–690.
- (16) Shintani, H.; Tanaka, H. *Nature Phys.* **2006**, *2*, 200.
- (17) Adrjanowicz, K.; Kaminski, K.; Wojnarowska, Z.; Dulski, M.; Hawelek, L.; Pawlus, S.; Paluch, M.; Sawicki, W. *J. Phys. Chem B* **2010**, *114*, 6579–6593.
- (18) Wojnarowska, Z.; Adrjanowicz, K.; Włodarczyk, P.; Kaminska, E.; Kaminski, K.; Grzybowska, K.; Wrzalik, R.; Paluch, M.; Ngai, K. L. *J. Phys. Chem B* **2009**, *113*, 12536–12545.
- (19) Sanz, A.; Nogales, A.; Ezquerro, T. A. *Macromolecules* **2010**, *43*, 29–32.

- (20) Kohlrausch, R. *Ann. Phys.* **1847**, 72, 393–404. Williams, G.; Watts, D. C. *Trans. Faraday Soc.* **1970**, 66, 80–85.
- (21) Kamiński, K.; Kamińska, E.; Pawlus, S.; Włodarczyk, P.; Paluch, M.; Ziolo, J.; Kasprzycka, A.; Szeja, W.; Ngai, K. L.; Pilch, J. *Carbohydr. Res.* **2009**, 344, 2547–2553.
- (22) Havriliak, S.; Negami, S. *J. Polym. Sci., Part C* **1966**, 14, 99.
- (23) (a) Vogel, H. *Phys. Z.* **1921**, 22, 645–646. (b) Fulcher, G. *J. Am. Ceram. Soc.* **1925**, 8, 339–355. (c) Tammann, G.; Hesse, W. *Z. Anorg. Allg. Chem.* **1926**, 156, 245–257.
- (24) Kamiński, K.; Włodarczyk, P.; Hawelek, L.; Adrjanowicz, K.; Wojnarowska, Z.; Paluch, M.; Kamińska, E. *Phys. Rev. E* **2011**, 83, 061506.
- (25) Bottcher, C. *Theory of Dielectric Polarization*; Elsevier Scientific Publishing Company: Amsterdam, 1973.
- (26) Kremer, F.; Schonhals, A. *Broadband Dielectric Spectroscopy*; Springer: New York, 2002.
- (27) Avrami, M. *J. Chem. Phys.* **1940**, 8, 212–224.
- (28) Avrami, M. *J. Chem. Phys.* **1939**, 7, 1103–1112.
- (29) Wunderlich, B. *Macromolecular Physics. Crystal Nucleation, Growth, Annealing*; Academic Press: London, 1976; Vol. 2.
- (30) (a) Meares, P. *Polymers, Structure and Bulk Properties*; Van Nostrand: London, 1965. (b) Cowie, J. M. G. *Polymers, Chemistry and Physics of Modern Materials*; Blackie: Glasgow, England, 1991.
- (31) Avramov, I.; Avramova, K.; Russel, C. *J. Cryst. Growth* **2005**, 285, 394–399.
- (32) Napolitano, S.; Wubbenhorst, M. *J. Phys.: Condens. Matter* **2007**, 19, 205121.
- (33) Napolitano, S.; Wubbenhorst, M. *J. Non-Cryst. Solids* **2007**, 353, 4357–4361.
- (34) Vyazovkin, S. *New J. Chem.* **2000**, 24, 913–917.
- (35) Sidebottom, D. L. *Phys. Rev. E* **2007**, 76, 011505.
- (36) *Methods in Carbohydrate Chemistry*; Whistler, R. L., Wolfrom, M. L., Eds.; Academic Press: New York, 1963; Vol. II, p 212.